Paper presentation

Building Block Metal Nanocluster-Based Growth in 1D Direction

Yao Qiao, Jiafeng Zou, Wenwen Fei ✉, Wentao Fan, Qing You, Yan Zhao, Man-Bo Li ✉, Zhikun Wu ✉

Published on: 17.10.2023   https://doi.org/10.1002/smll.202305556

Zhikun Wu: Institute of Solid State Physics, Hefei Institute of Solid State Physics, Chinese Academy of Sciences, Hefei, China

Man-Bo Li, Wenwen Fei: Institute of Physical Science and Information Technology, Anhui University, Hefei, China

Key Laboratory of Materials Physics, Anhui Key Laboratory of Nanomaterials and Nanotechnology, CAS Center for Excellence in Nanoscience, Institute of Solid State Physics, Hefei Institutes of Physical Science (HFIPS), Chinese Academy of Sciences, Hefei, China
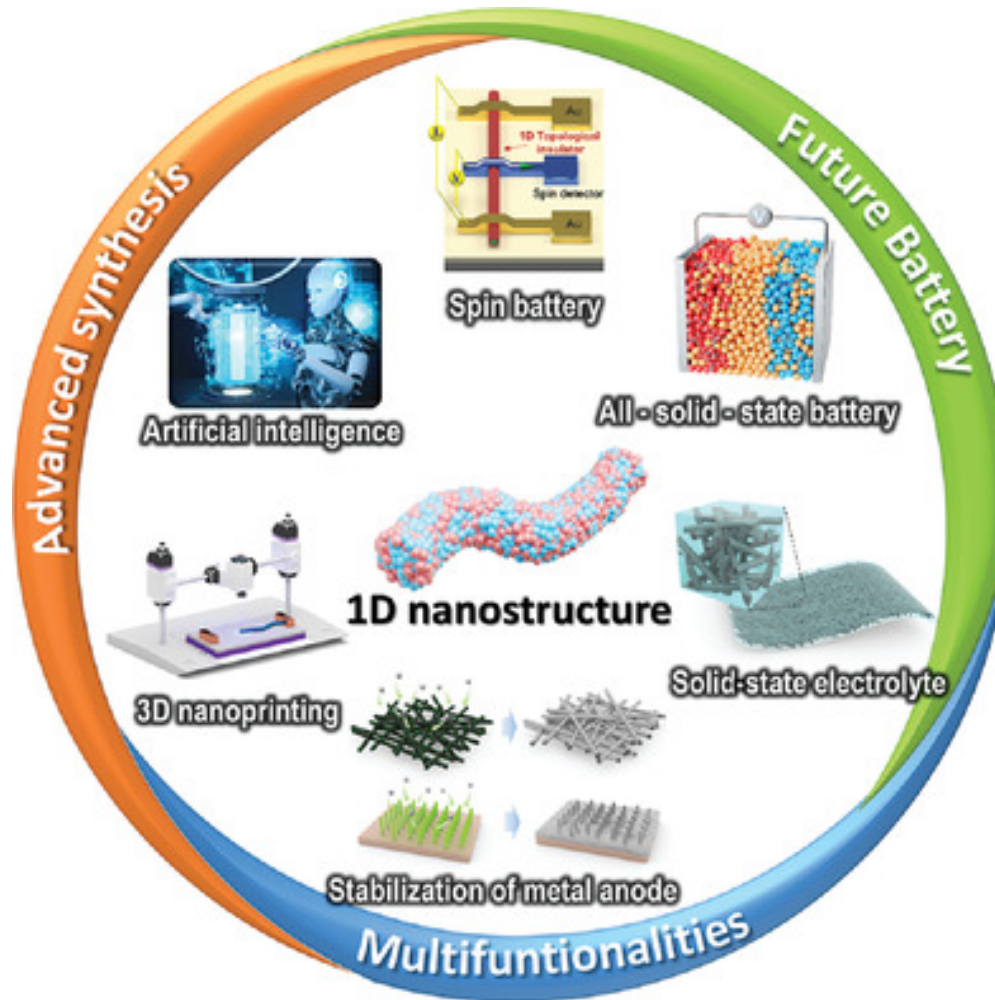
Samapti Mondal

02.03.2024

1

Introduction

1D linear growth of building blocks $\longrightarrow$ Nanomaterials with specific structures


Atomic precision

Defined structures

Cheong, J. Y., et al., *Adv. Funct. Mater.* **2022**, *32*, 2208374

Background

Article | Open access | Published: 28 March 2023

Key factors for connecting silver-based icosahedral superatoms by vertex sharing

Sayuri Miyajima, Sakiat Hossain ✉, Ayaka Ikeda, Taiga Kosaka, Tokuhisa Kawawaki, Yoshiki Niihori, Takeshi Iwasa ✉, Tetsuya Taketsugu & Yuichi Negishi ✉
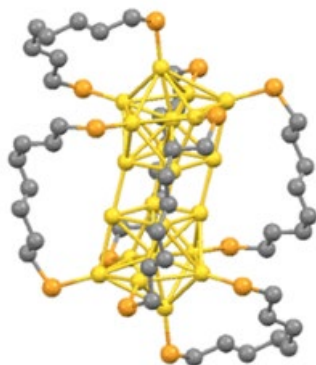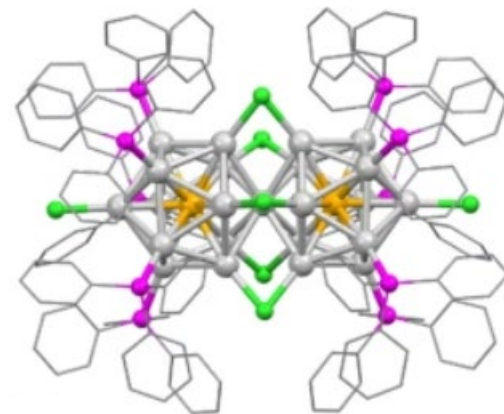
Controlling Gold Nanoclusters by Diphospine Ligands

Jing Chen, Qian-Fan Zhang, Timary A. Bonaccorso, Paul G. Williard, and Lai-Sheng Wang*

View Author Information ∨

Article Views	Altmetric	Citations
5392	2	212

LEARN ABOUT THESE METRICS

Size Growth of Au$_4$Cu$_4$: From Increased Nucleation to Surface Capping

Zidong Lin, Ying Lv, Shan Jin*, Haizhu Yu*, and Manzhou Zhu*

Article Views	Altmetric	Citations
1678	1	-

LEARN ABOUT THESE METRICS

3
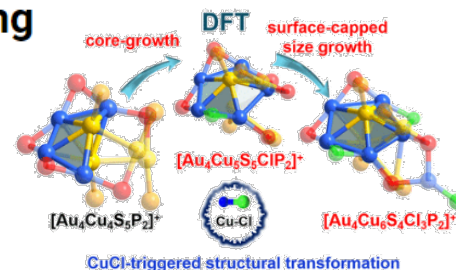
Background

Gold Nanowired: A Linear $(Au_{25})_n$ Polymer from Au_{25} Molecular Clusters

Marco De Nardi[†], Sabrina Antonello[†], De-en Jiang[‡], Fangfang Pan[§], Kari Rissanen[§], Marco Ruzzi[†], Alfonso Venzo[†⊥], Alfonso Zoleo[†], and Flavio Maran[†*]

View Author Information ⌄

Assembly-induced spin transfer and distance-dependent spin coupling in atomically precise AgCu nanoclusters

Nan Xia, Jianpei Xing, Di Peng, Shiyu Ji, Jun Zha, Nan Yan, Yan Su, Xue Jiang, Zhi Zeng ✉, Jijun Zhao ✉ & Zhikun Wu ✉
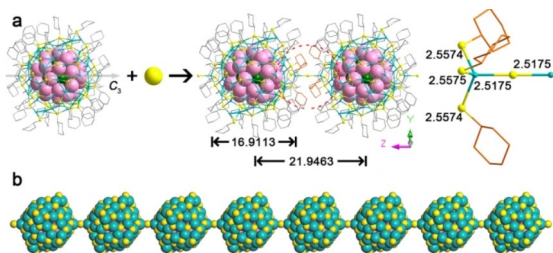
Why this paper?

- ✓ It shows controllable linear growth of NC in a one-dimensional direction in three different fashions by tuning the reaction conditions.

- ✓ It also provides an in-depth investigation of the growth mechanism of formation of such 1D nanomaterials.

- ✓ The shoulder-to-shoulder fusion of Au_{13} building blocks to form Au_{33} NC is achieved for the first time from an experimental perspective.

In this paper

$[Au_{13}Cd_2(SCH_2CH_2Ph)_6(PPh_3)_6(NO_3)_2]^+$

[icosahedron] $(Au_{13}Cd_2)_2O$

9.8302 Å

Dimer

"Hand-in-Hand" Linear Growth

[icosahedron] rod-like Au_{25}

"Head-to-Head" Linear Growth

"Shoulder-to-Shoulder" Linear Growth

[cuboctahedron] Au_{33}
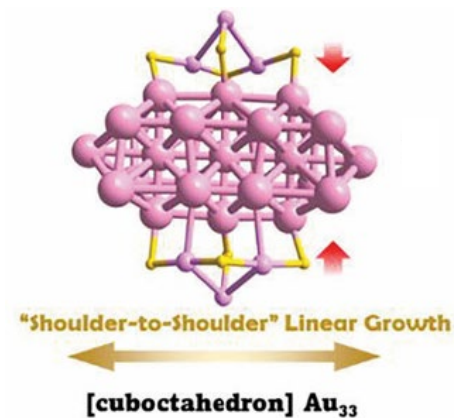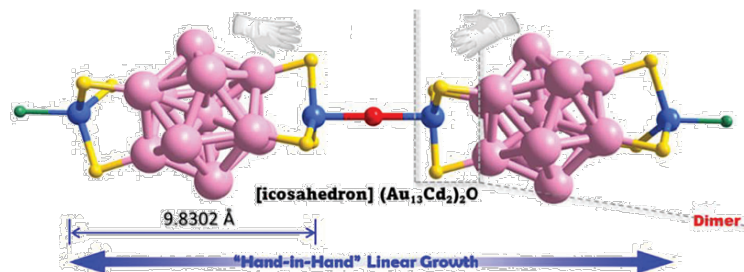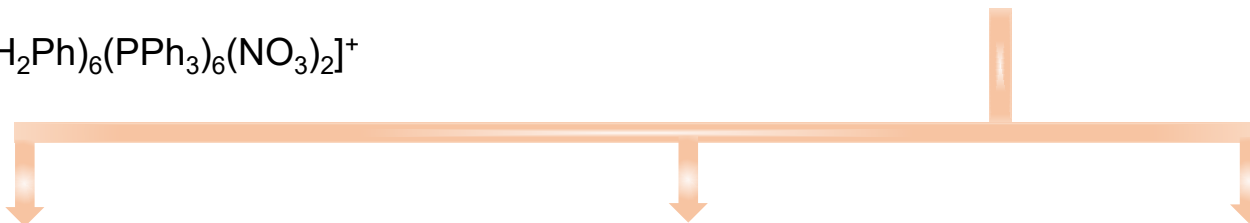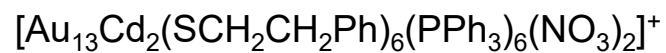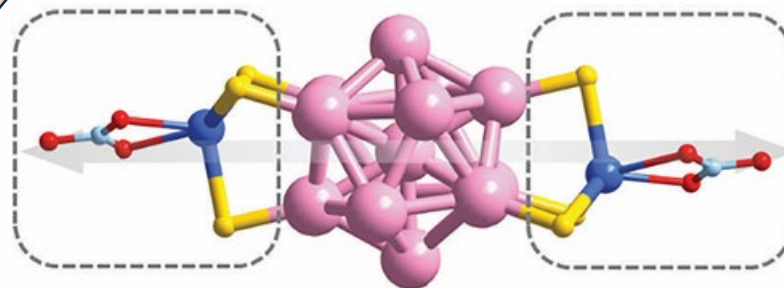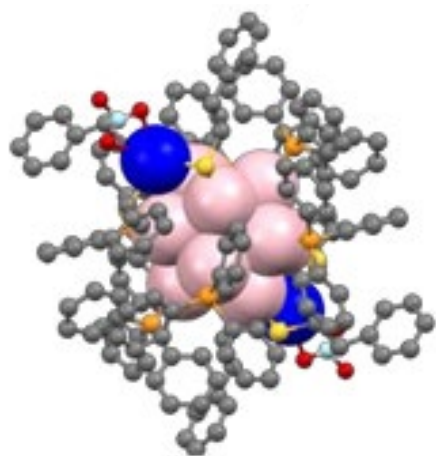
Results and discussion

Figure 1. a) The unique structure of the parent nanocluster "$Au_{13}Cd_2$-TPP-NO_3"; b–d) the photographs, UV–vis and ESI-MS spectra of the reaction of $Au_{13}Cd_2$-TPP-NO_3 under different conditions. The carbonaceous parts of thiolates and all triphenylphosphines are omitted for clarity. (Pink: Gold; Light blue: Cadmium; Yellow: Sulfide; Red: Oxygen; and Pale blue: Nitrogen).
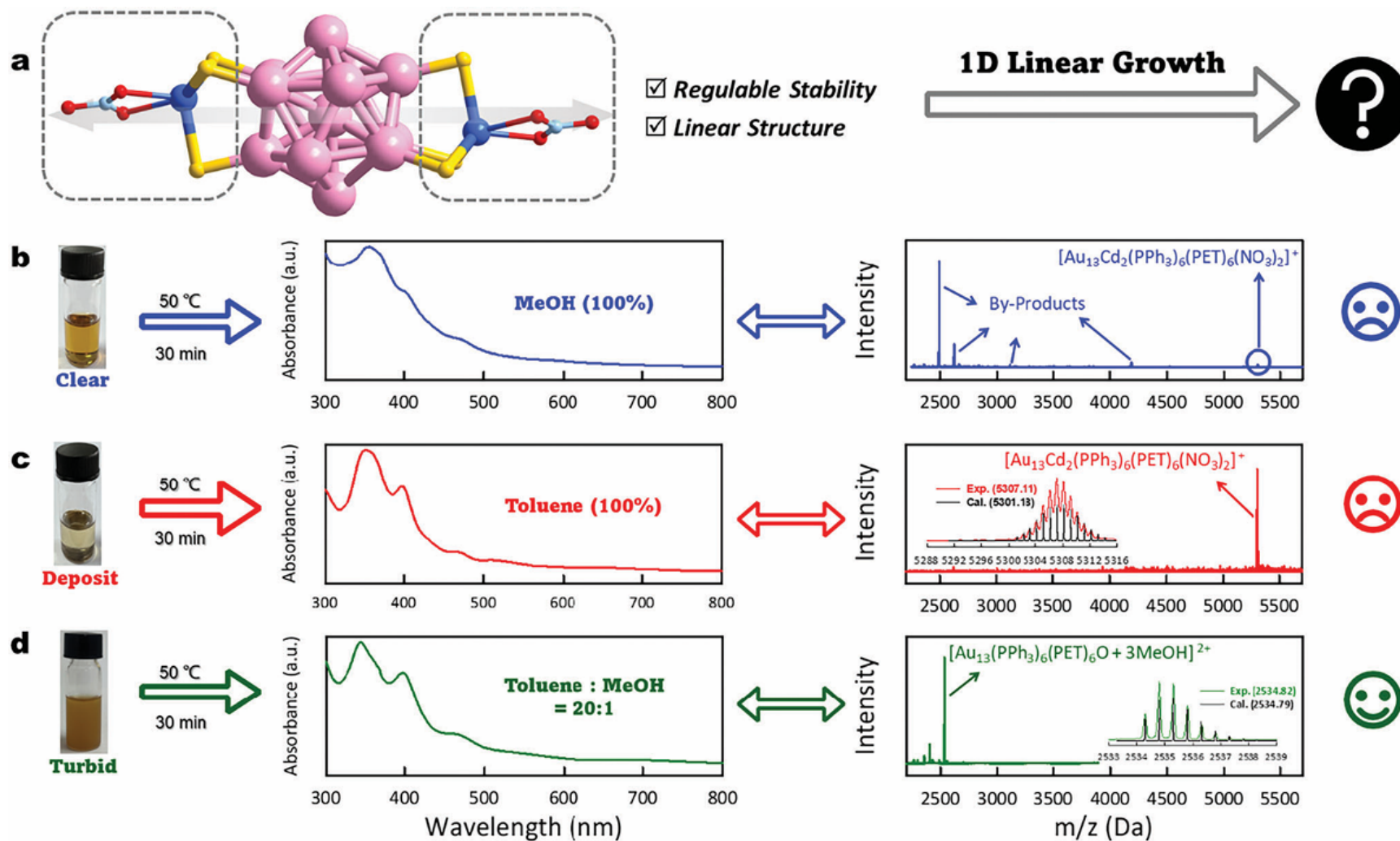
Results and discussion

Synthetic protocol used to obtain 'hand-in-hand' 1D growth:

$Au_{13}Cd_2$-TPP-NO_3 (10 mg)
+
20 mL toluene + 1 mL MeOH

↓ Sonicated for 1 min
50 $^\circ$C ,30 min,
500 rpm

Crude product of dimeric $Au_{13}Cd_2$

↓ Washed with hexane
Crystallized in 1:1 DCM-Hexane,
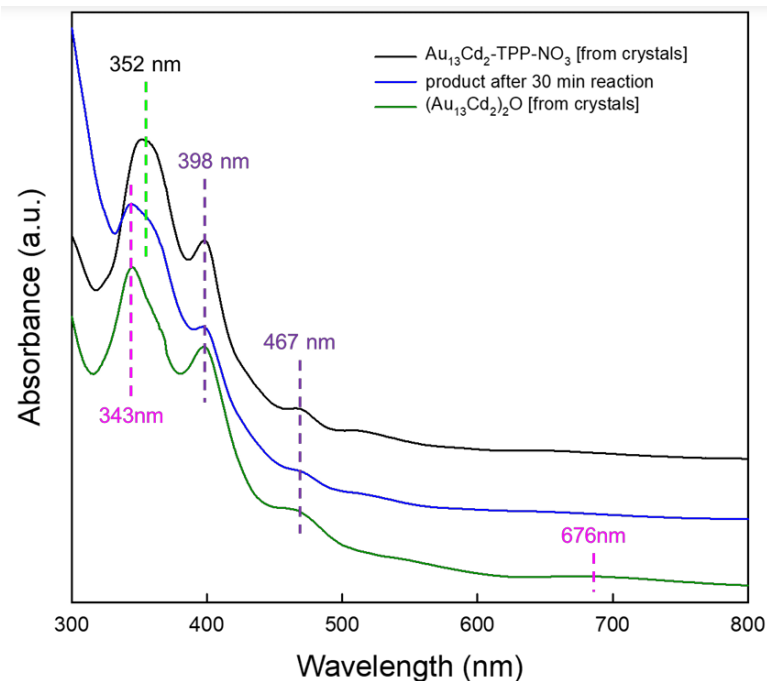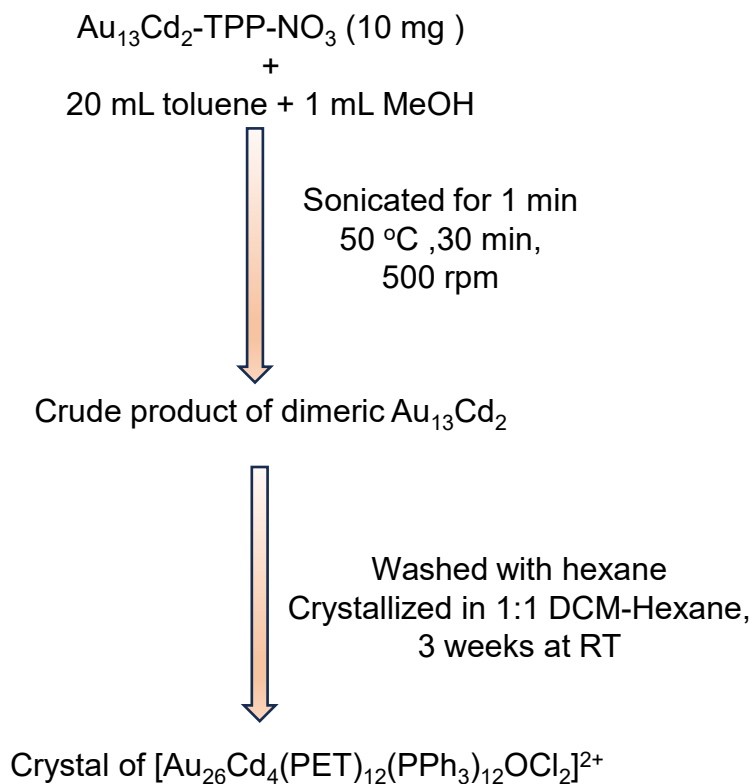3 weeks at RT

Crystal of $[Au_{26}Cd_4(PET)_{12}(PPh_3)_{12}OCl_2]^{2+}$

Figure S3. The comparison of UV-vis spectra of $Au_{13}Cd_2$-TPP-NO_3, product after 30 min reaction, and $(Au_{13}Cd_2)_2O$

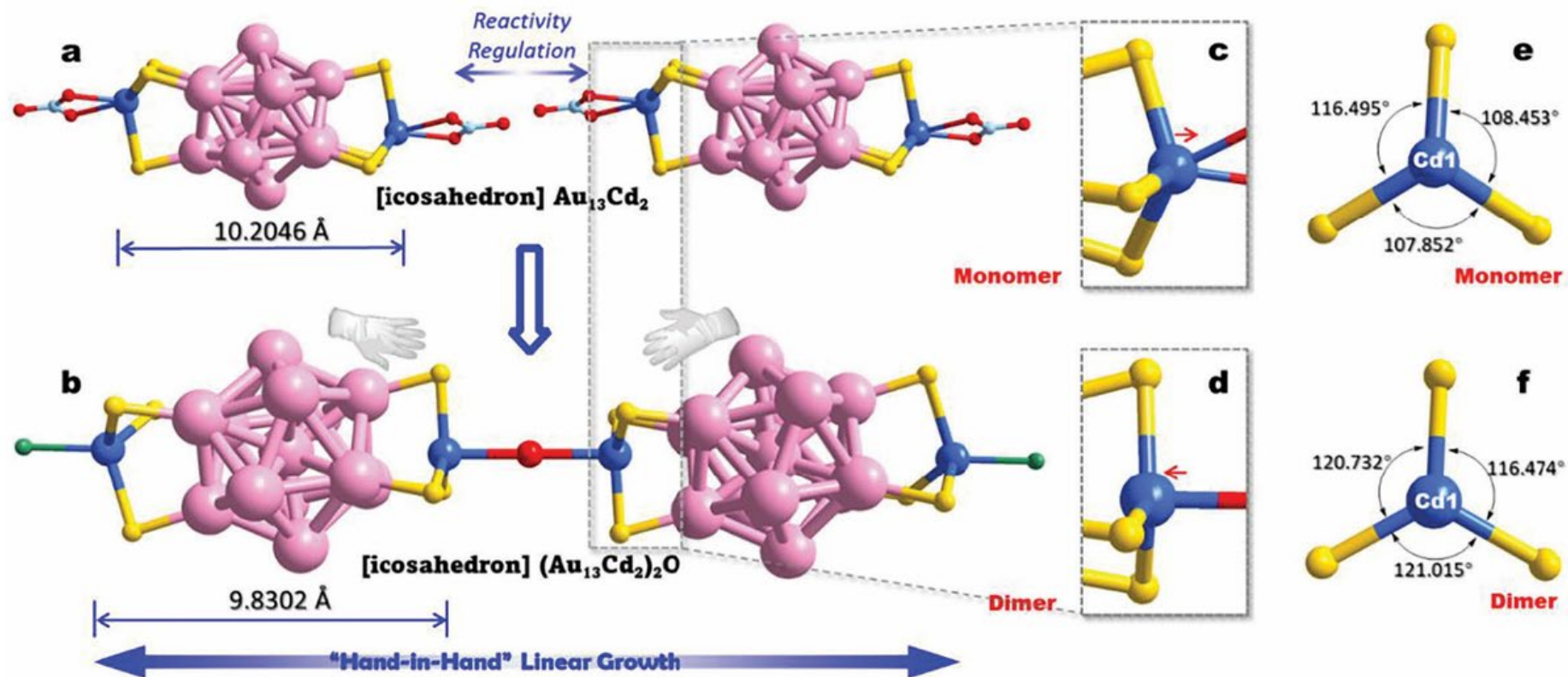**Figure 2**. a,b) Illustration of the "Hand-in-hand" ID growth of $Au_{13}Cd_2$-TPP-NO_3 for synthesizing $(Au_{13}Cd_2)_2O$ nanocluster. c,d) The relative position of S and Cd atoms in $Au_{13}Cd_2$-TPP-NO_3 and $(Au_{13}Cd_2)_2O$ nanoclusters. e,f) The "S-CdI-S" angles of $Au_{13}Cd_2$-TPP-NO_3 and $(Au_{13}Cd_2)_2O$ nanoclusters.

Results and discussion
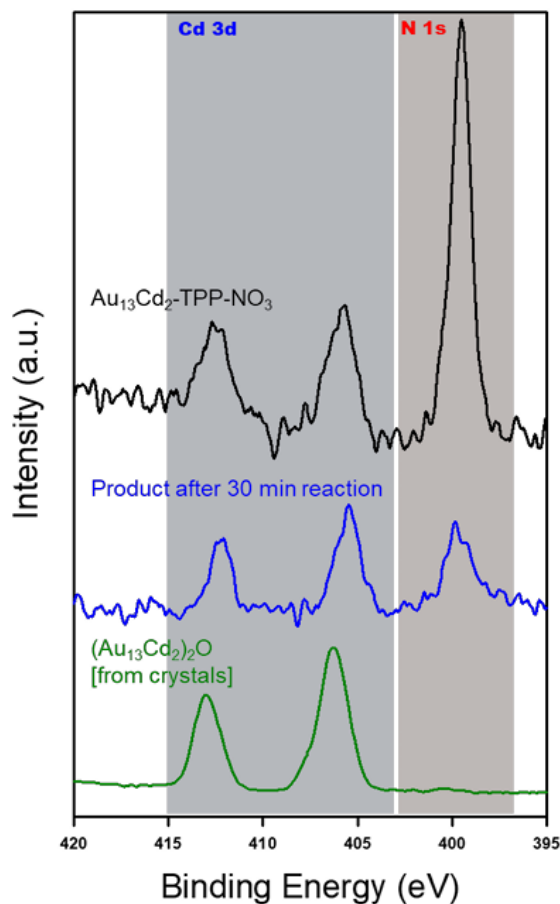

Figure S6. High-resolution XPS survey scans of Cd 3d and N 1s of the dimeric $(Au_{13}Cd_2)_2O$ nanocluster, the product after 30 min reaction, and $(Au_{13}Cd_2)_2O$

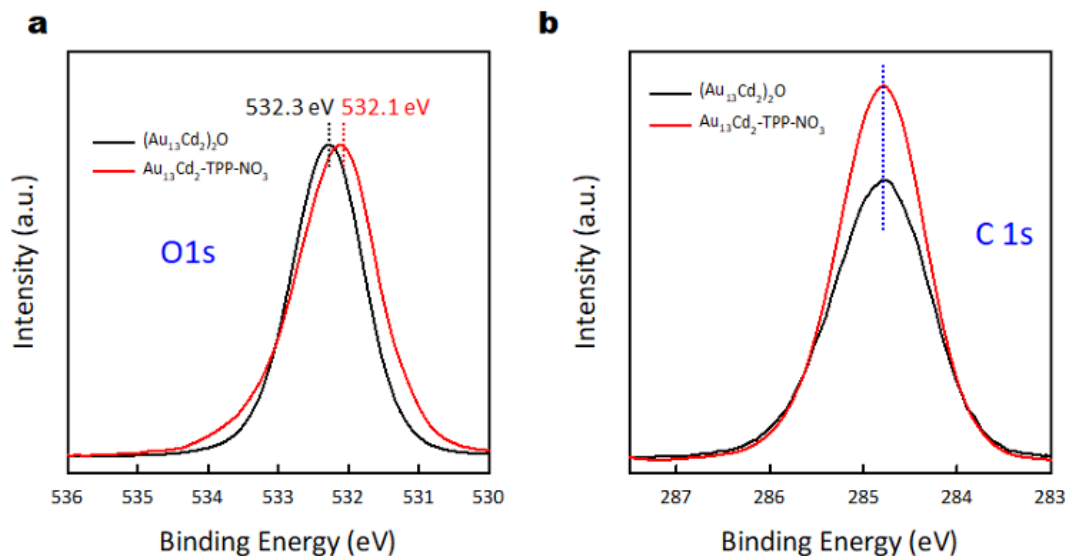**Figure S5**. High-resolution XPS survey scans of O 1s (a) and C 1s (b) of the dimeric $(Au_{13}Cd_2)_2O$ nanocluster (black) and the monomeric $Au_{13}Cd_2$-TPP-NO_3 nanocluster

Results and discussion

Investigation of the mechanism

1D growth of $(Au_{13}Cd_2)O$ 👉 instability of $Cd_2(PET)_3NO_3$ claw-like motif in $Au_{13}Cd_2$-TPP-NO_3
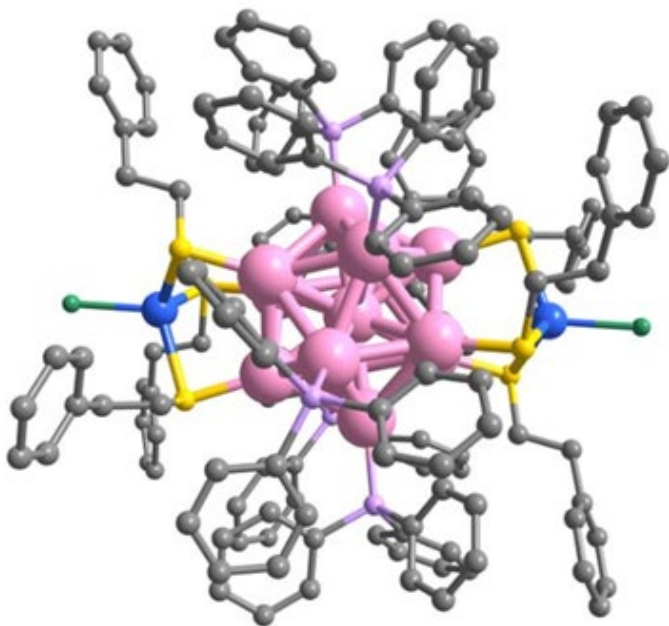
Figure S9. X-ray crystal structure of $Au_{13}Cd_2$-TPP-Cl nanocluster.
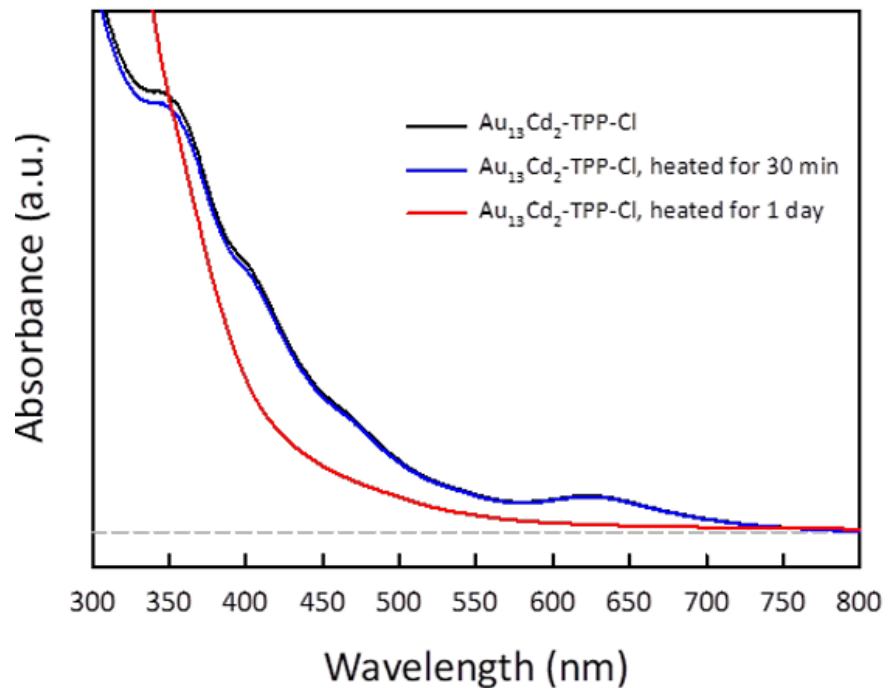
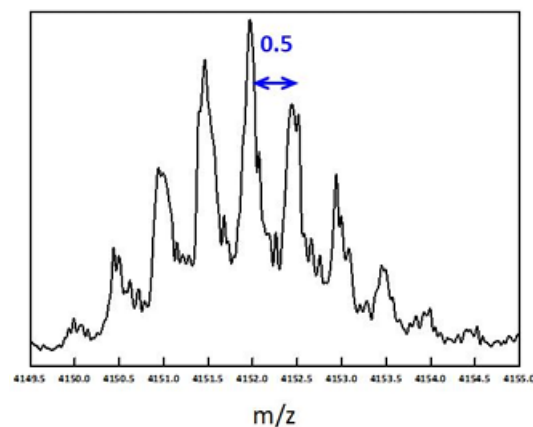**Figure S10**. UV-vis spectra of the freshly prepared $Au_{13}Cd_2$-TPP-Cl nanocluster, after heating for 30 minutes, and for one day.

Results and discussion

1D growth of the parent cluster in the dissolved state: head-to-head fusion of Au_{13}

Synthetic protocol used to obtain 'head-to-head' 1D growth:

$Au_{13}Cd_2$-TPP-NO_3 (10 mg)
+
20 mL MeOH

↓ 50 °C ,30 min
10 uL HCl (37%)

After 12 h at RT,
Quenched with
100 mL deionized
water

Washed with hexane
Crystallized in 1:1 DCM-
Hexane, 1 week at 0 °C

Crystal of $[Au_{25}(PET)_5(PPh_3)_{10}Cl_2]^{2+}$
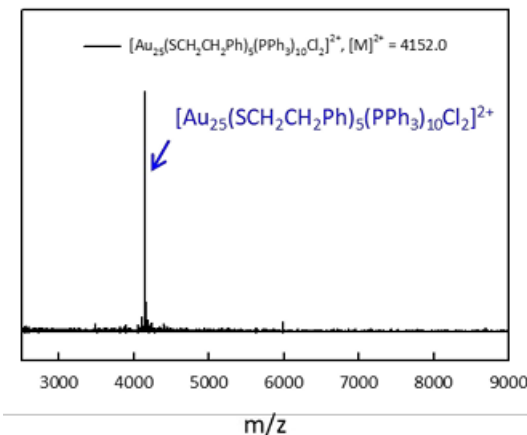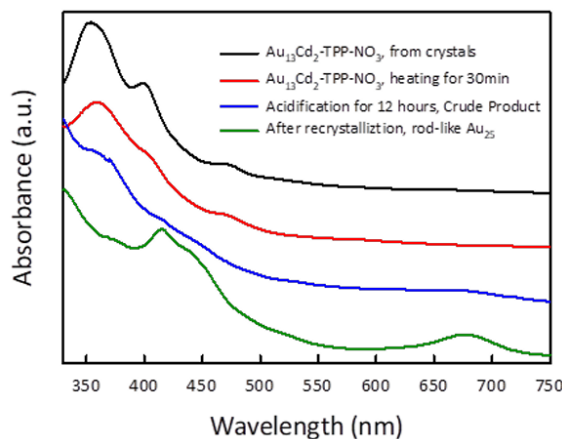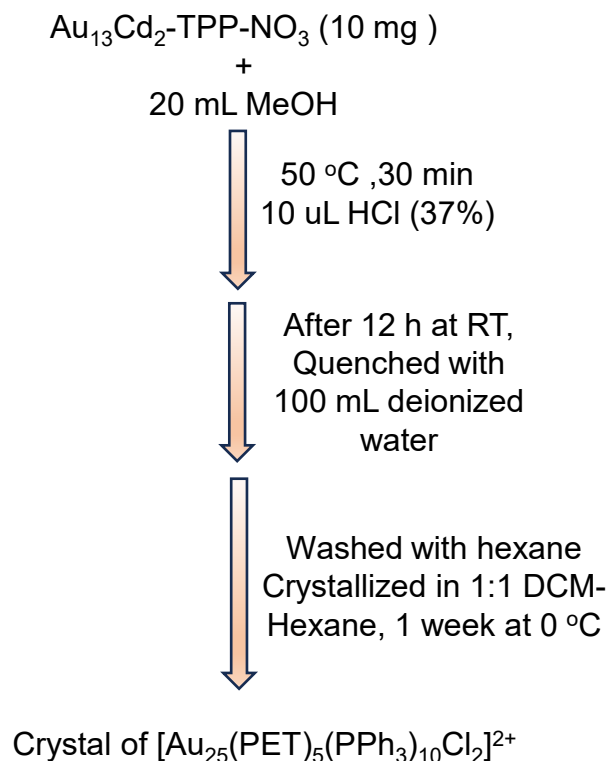
Results and discussion
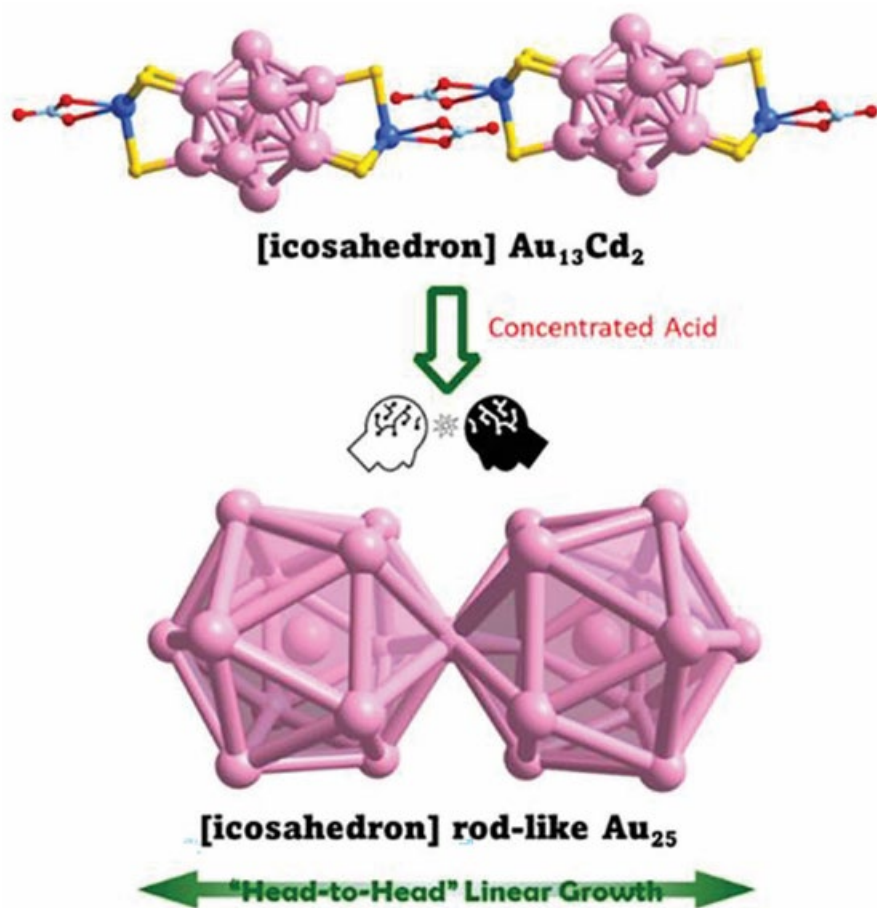
Figure 3. "Head-to-head" 1D growth of $Au_{13}Cd_2$-TPP-NO_3 for synthesizing $[Au_{25}(PET)_5(PPh_3)_{10}Cl_2]^{2+}$ nanocluster.

Figure S12. X-ray crystal structure of $[Au_{25}(PET)_5(PPh_3)_{10}Cl_2]^{2+}$ nanocluster
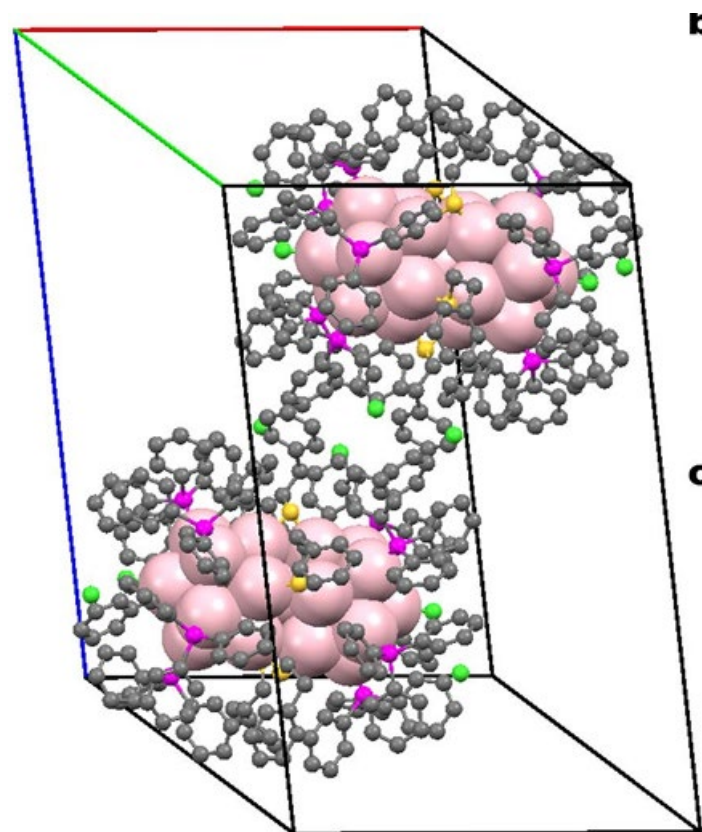
13

Results and discussion

Evolution of 1D 'shoulder-to-shoulder' growth

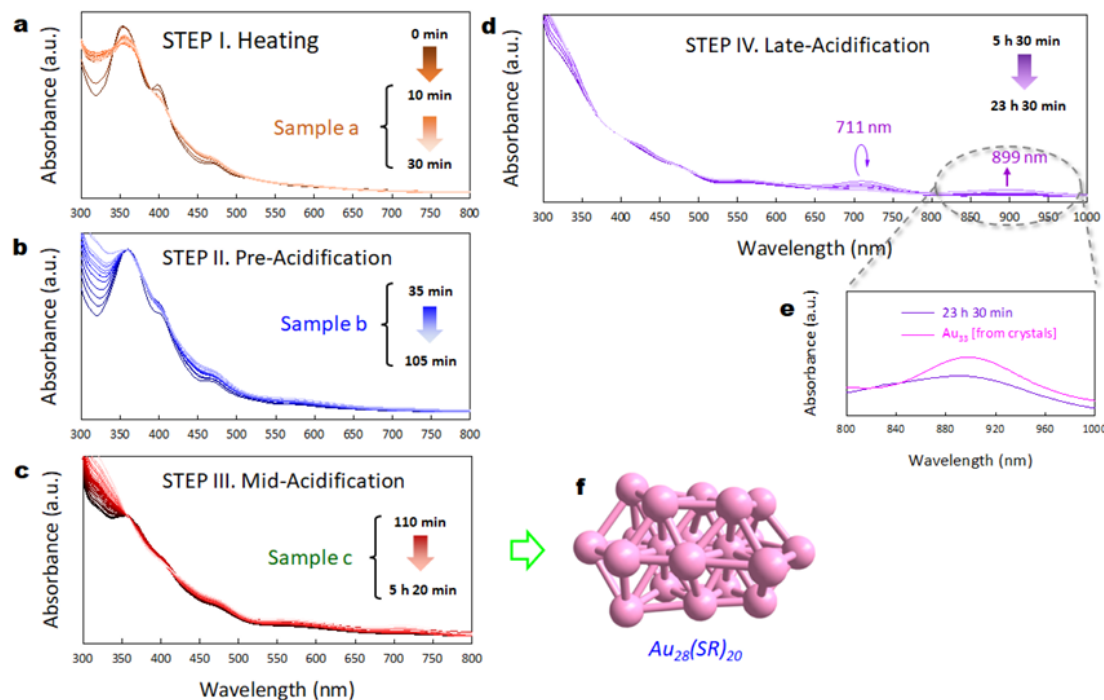

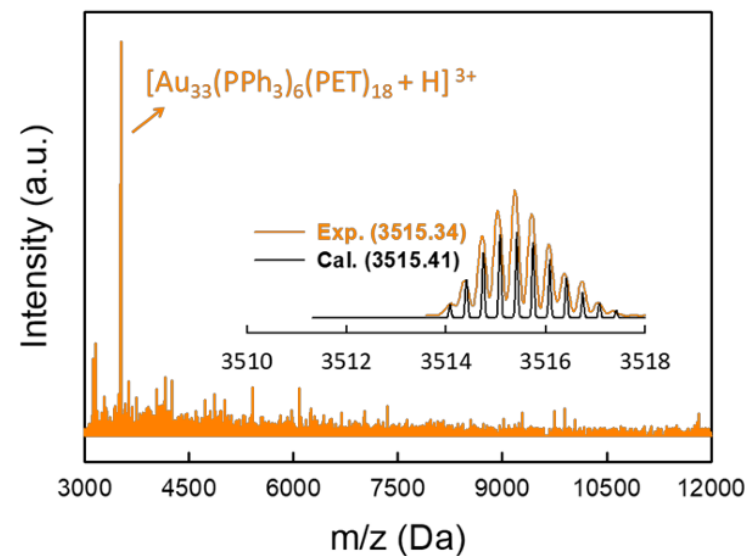**Figure S14**. The formation process of Au$_{33}$ nanocluster.

Figure S15. ESI-MS spectrum of the Au$_{33}$ nanocluster (positive-ion mode).
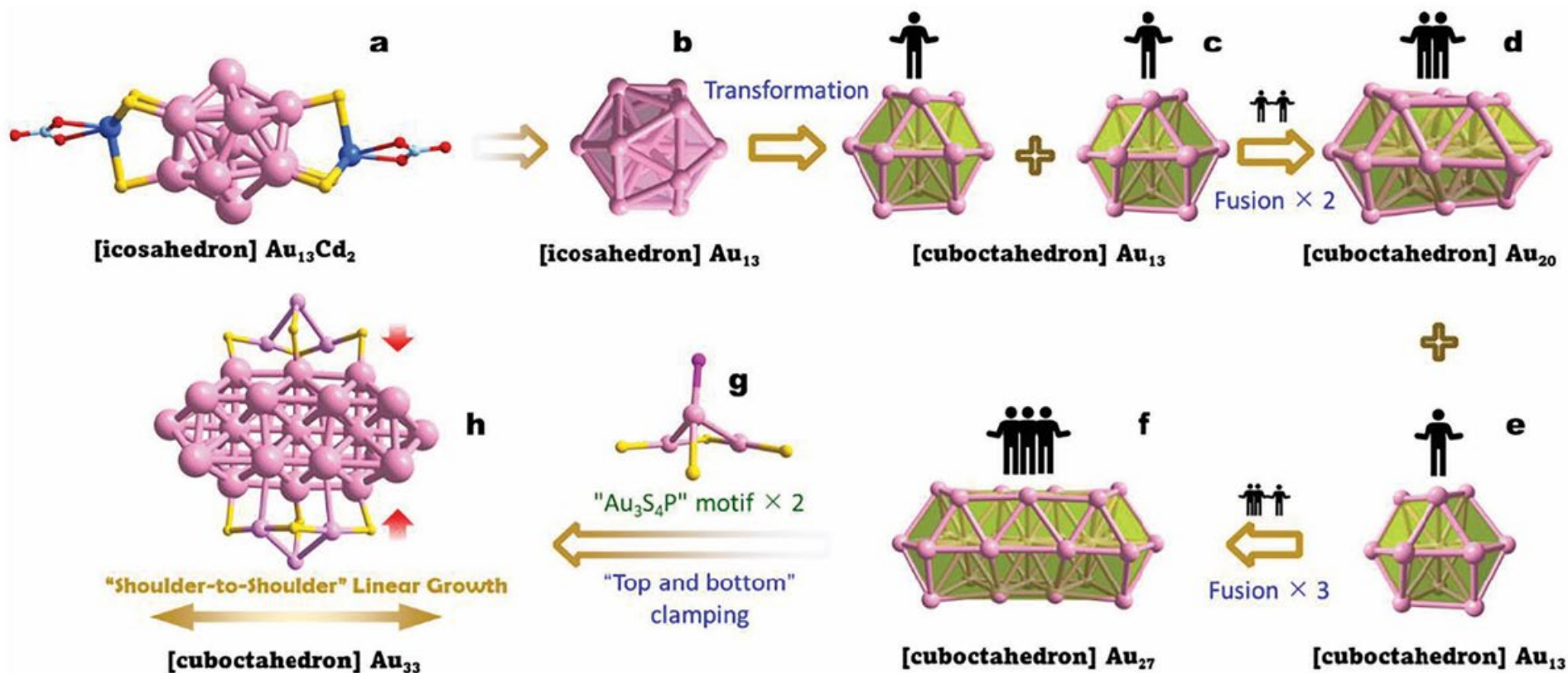
Results and discussion

Figure 4. Illustration of the initial Cd exclusion (a,b), the subsequential kernel growth (c–f), and the final formation of Au_{33} of the "Shoulder-to-shoulder" 1Dgrowth of $Au_{13}Cd_2$-TPP-NO_3 nanocluster.

Results and discussion

Investigation of the possible growth pathway of Au_{33}

Step-I: heating (25 min) →crystallization→ $Au_{13}Cd_2$-TPP-NO_3

⇩

Step-II: Pre-acidification (100 min)

⇩

Step-III: Mid-acidification (3 h) →crystallization→ $Au_{28}S_{20}$
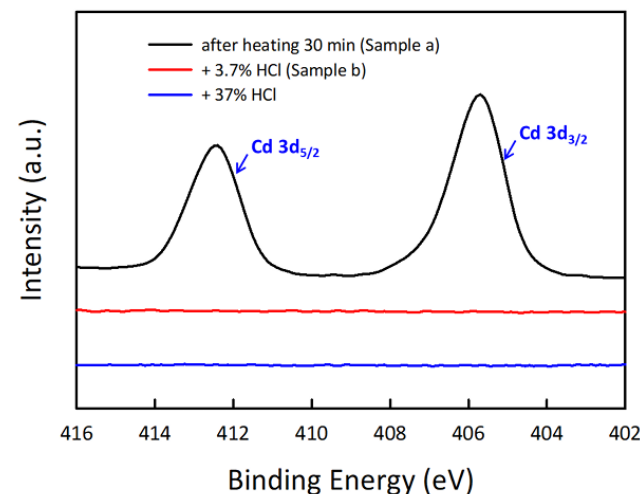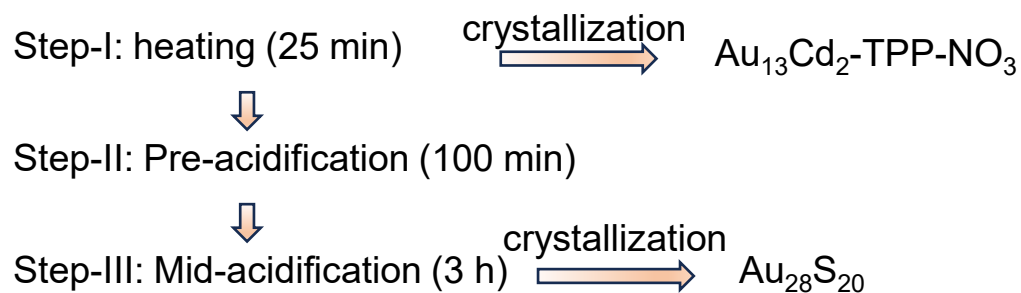

Figure S22. High-resolution XPS survey scans of Cd 3d of Sample a (black) and b (red).
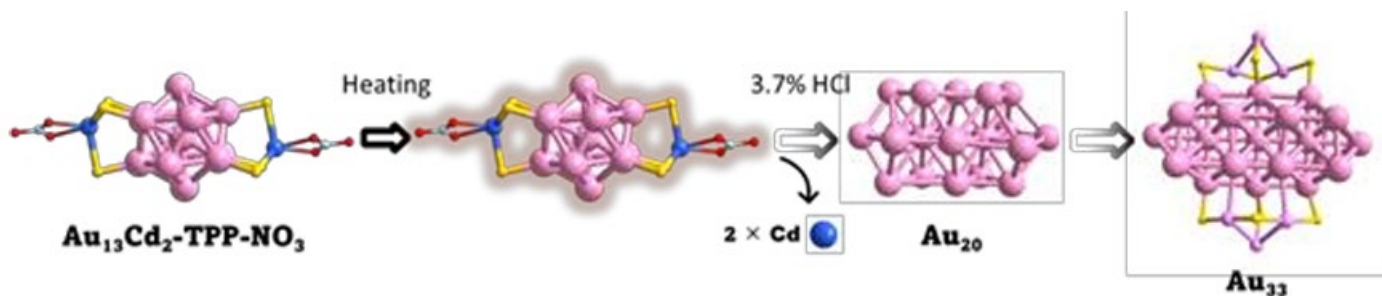

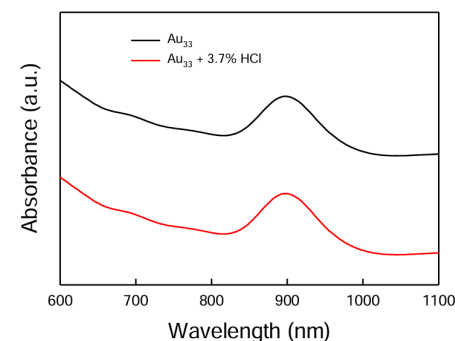**Figure S24**.The proposed growth mechanism of Au_{33} nanocluster.

Figure S25. The UV-vis spectra of Au_{33} and after adding diluted acid.
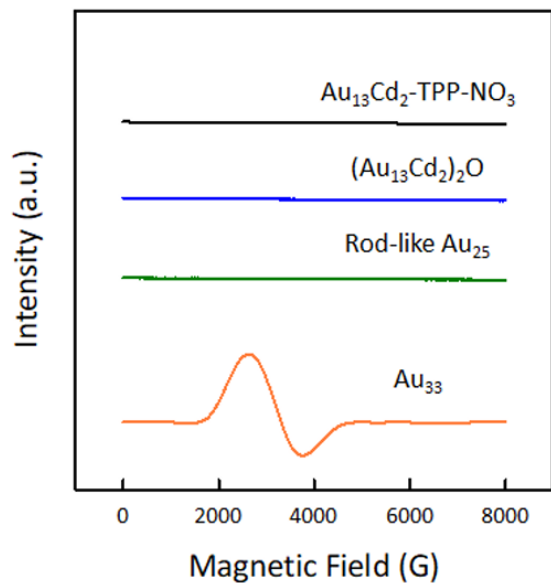
Results and discussion

Figure S14. EPR spectra of $Au_{13}Cd_2$-TPP-NO_3 $(Au_{13}Cd_2)_2O$, rod-like Au_{25}, and Au_{33} nanoclusters.
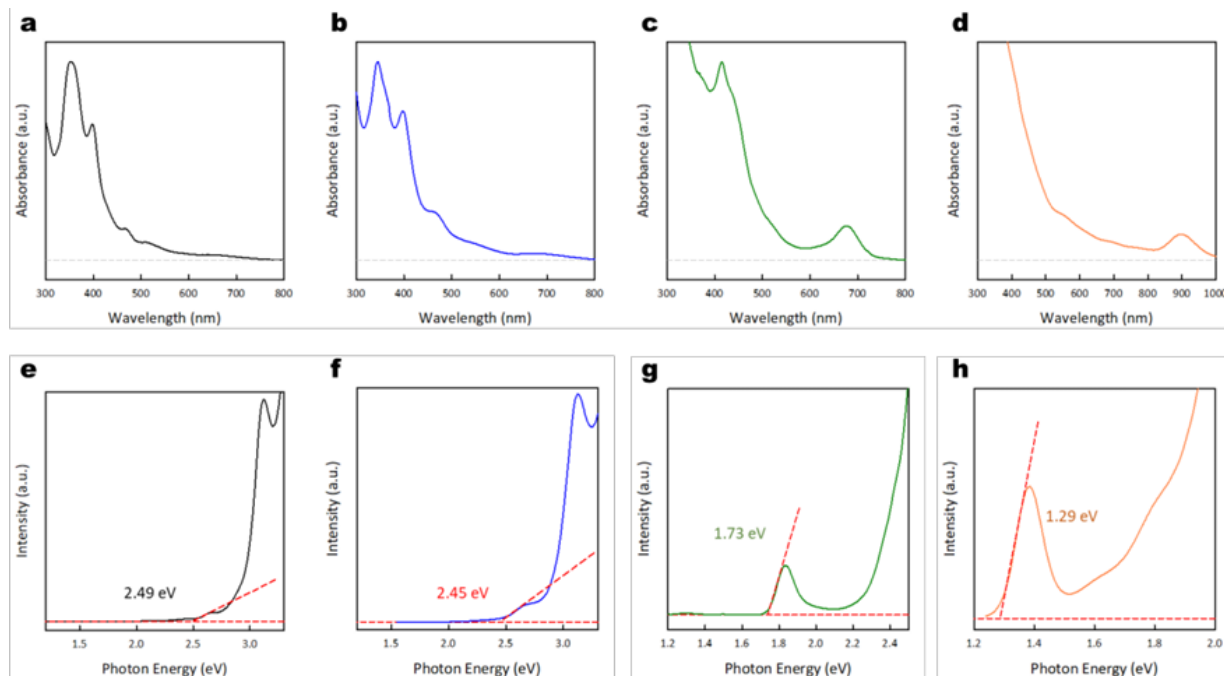
Figure S14. UV-vis spectra and photo-energy plots of $Au_{13}Cd_2$-TPP-NO_3 (a, e), $(Au_{13}Cd_2)_2O$ (b, f), rod-like Au_{25} (c, g), and Au_{33} (d, h) nanoclusters.

From the calculation of the frontier orbitals, the HOMO-LUMO gap (Eg) of the Au NCs: $Au_{13}Cd_2$-TPP-NO_3 (2.48eV) > $(Au_{13}Cd_2)_2O$ (2.42 eV) > Au_{25} (1.54 eV) > Au_{33} (1.42 eV)

Conclusion

- In this study, selective 1D growth of $Au_{13}Cd_2$ building block nanocluster into three different linear nanoclusters by tuning the reaction condition has been explored.

- The dimeric $(Au_{13}Cd_2)_2O$ NC is grown in a hand-in-hand fashion by adjusting the solubilities of the parent NC.

- The Au_{25} has originated by exposing the parent cluster to strong acidic conditions whereas the Au_{33} is formed by shoulder-to-shoulder fusion under the weak acidic condition.

- The compositions and structures were investigated through SCXRD and other characterizations.

- The growth mechanism of the formation of those species has been investigated through XPS, UV-vis, and SCXRD studies.

- Electron Paramagnetic Resonance and DFT calculations show that the unpaired valence electron and narrow band gap (1.42 eV) of the Au_{33} nanocluster reveal its potential as a semiconducting or magnetic material.